HHS Public Access

Author manuscript

Nat Immunol. Author manuscript; available in PMC 2016 July 04.

Published in final edited form as:

Nat Immunol. 2016 February ; 17(2): 187–195. doi:10.1038/ni.3327.

Polyclonal CD4+ T cell tolerance is established by distinct mechanisms, according to self-peptide expression patterns

Deepali Malhotra[1], **Jonathan L. Linehan**[1,6], **Thamotharampillai Dileepan**[1], **You Jeong Lee**[2], **Whitney E. Purtha**[5], **Jennifer V. Lu**[5], **Ryan W. Nelson**[1], **Brian T. Fife**[3], **Harry T. Orr**[4], **Mark S. Anderson**[5], **Kristin A. Hogquist**[2], and **Marc K. Jenkins**[1,7]

[1]Department of Microbiology and Immunology, Center for Immunology, University of Minnesota Medical School, Minneapolis, MN, USA, 55455

[2]Department of Laboratory Medicine and Pathology, Center for Immunology, University of Minnesota Medical School, Minneapolis, MN, USA, 55455

[3]Department of Medicine, Center for Immunology, University of Minnesota Medical School, Minneapolis, MN 55455

[4]Department of Laboratory Medicine and Pathology, Institute for Translational Neuroscience, University of Minnesota Medical School, Minneapolis, MN, USA, 55455

[5]Diabetes Center, University of California San Francisco, San Francisco, CA, USA, 94143

Abstract

Studies of mouse monoclonal CD4$^+$ T cell repertoires have revealed several mechanisms of self-tolerance, however, which mechanisms operate in normal repertoires is unclear. Here, polyclonal CD4$^+$ T cells specific for green fluorescent protein expressed in different organs were studied, allowing determination of the effects of specific expression patterns on the same epitope-specific T cells. Peptides presented uniformly by thymic antigen-presenting cells were tolerated by clonal deletion, whereas thymus-excluded peptides were ignored. Peptides with limited thymic expression induced partial clonal deletion and impaired effector but enhanced regulatory T cell potential. These mechanisms were also active for T cell populations specific for endogenously expressed self-antigens. Thus, immune tolerance of polyclonal CD4$^+$ T cells is maintained by distinct mechanisms, according to self-peptide expression patterns.

[7]To whom correspondence should be addressed: ; Email: jenki002@umn.edu

[6]Current address: Laboratory of Parasitic Diseases, NIAID, NIH, Bethesda, MD.

AUTHOR CONTRIBUTIONS

D. M. designed the study, did experiments, analyzed data, and wrote the manuscript, J. L. L, T. D., Y. J. L., R.W.N., W.E.P., J.V.P., and M. S. A. did experiments, K. A. H., B.T.F., and H. T. O. provided discussion, M. K. J. designed the study, analyzed data, and wrote the manuscript.

COMPETING FINANCIAL INTERESTS

The authors declare no competing financial interests.

Keywords

CD4+ T lymphocyte; immunological tolerance; clonal deletion; immunological ignorance

Self-reactive CD4+ T cells are generated in the normal course of T cell receptor (TCR) rearrangement[1]. Low affinity interactions between TCR and self-peptide-major histocompatibility class II (self-peptide:MHCII) ligands are essential for positive selection of T cells in the thymus[1]. High affinity TCR-self-peptide:MHCII interactions, however, can cause autoimmunity. Therefore, tolerance mechanisms have evolved to limit T cells with TCRs with high affinities for self-peptide:MHCII ligands.

Different tolerance mechanisms may be engaged depending on where a self-peptide:MHCII epitope is displayed. A developing thymocyte may die by apoptosis or differentiate into a regulatory T cell (T_{reg} cell) if its TCR binds strongly to a self-peptide:MHCII epitope displayed on particular antigen-presenting cells[1, 2]. Epitopes in this class may be derived from proteins expressed or taken up by MHCII+ thymic epithelial cells or dendritic cells. However, MHCII+ cells in the thymus might not display epitopes from all host proteins. Thus, T cells expressing TCRs with high affinities for certain self-epitopes may not be deleted in the thymus and exit to secondary lymphoid organs[2, 3, 4, 5, 6]. Some T cells in this class may be specific for epitopes from proteins that are not secreted or are expressed in locations with poor lymphatic drainage. Since these proteins would not reach antigen-presenting cells in secondary lymphoid organs, specific T cells would be retained in the repertoire in a fully responsive state of ignorance[7, 8]. Other tissue-restricted proteins that are secreted or found in dying cells may reach secondary lymphoid organs where they would be processed by antigen-presenting cells to form self-peptide:MHCII epitopes. CD4+ T cells that encounter and recognize these epitopes may differentiate into T_{reg} cells[2] or become anergic due to a lack of innate immune system-derived costimulation[1, 9].

Much of the evidence cited above has come from studies of transgenic mice expressing monoclonal TCRs specific for self-peptide:MHCII epitopes[7, 8, 10]. These mice could reveal tolerance mechanisms because of the large numbers of T cells available for study. However, this approach has several limitations. Because a TCR transgenic mouse contains a single TCR from a larger repertoire, it can only reveal tolerance mechanisms that apply to TCRs with that affinity for a self-peptide:MHCII epitope[11]. Further, it is clear that an abundance of T cells with the same TCR can create abnormal outcomes[12, 13, 14]. This issue has come to the fore in several studies showing that clonal deletion is not as prominent a mechanism in polyclonal T cell repertoires as has been reported for certain monoclonal T cell populations [4, 5, 15]. These studies, however, have been limited to epitopes with ubiquitous patterns of expression.

A need therefore exists for a systematic study of tolerance within normal polyclonal CD4+ T cell repertoires specific for self-peptides with defined patterns of expression. Here, we carried out such a study using peptide:MHCII tetramer-based cell enrichment. Intrathymic deletion was the mechanism of tolerance for T cells specific for peptides from proteins expressed uniformly by thymic dendritic cells and/or medullary thymic epithelial cells, whereas ignorance was the mechanism for peptides from cytosolic or nuclear proteins

expressed only outside the thymus. Partial intrathymic deletion and impaired effector but enhanced T_{reg} cell potential among remaining clones was the mechanism for many peptides from tissue-restricted proteins that were also expressed sparsely in the thymus. Thus, $CD4^+$ T cells tolerate self-peptides with different expression patterns via different mechanisms.

RESULTS

eGFP transgenic mice model $CD4^+$ T cell tolerance to self

Enhanced green, yellow, or cyan fluorescent proteins (eGFP, eYFP, CFP) were used as model self-antigens in transgenic mouse strains expressing these proteins and the I-A^b MHCII molecule. These proteins contain an I-A^b-binding peptide (HDFFKSAMPEGYVQE, eGFPp), which was incorporated into an I-A^b tetramer that was used to detect $CD4^+$ T cells with TCRs specific for this epitope (Fig. 1a,b) [16]. This experimental system allowed determination of the effects of different patterns of self-antigen expression on the same epitope-specific T cell repertoire. Another advantage of this approach was that wild-type C57BL/6 (B6) mice, which express the I-A^b molecule but not eGFP, could be used as controls to study the relevant T cell repertoire in the absence of the self-peptide.

Tolerance in the eGFPp:I-A^b-specific $CD4^+$ T cell repertoire was examined by immunizing 14 different transgenic strains expressing eGFP, eYFP, or CFP (Supplementary table 1) with eGFPp in complete Freunds adjuvant (CFA). Single cell suspensions of secondary lymphoid organs from immunized mice were stained with the eGFPp:I-A^b tetramer labeled with allophycocyanin, then with anti-allophycocyanin-coated magnetic beads. Tetramer-bound cells were enriched on magnetized columns, eluted, and stained with antibodies designed to identify T cells. T_H1, T_H17, follicular helper (T_{FH}), and T_{reg} cell differentiation by the eGFPp:I-A^b-specific $CD4^+$ T cells was assessed by intracellular staining of the lineage-defining transcription factors T-bet (*Tbx21*), RORγt (*Rorc*), Bcl-6, and Foxp3, respectively (Fig. 1c).

Wild-type B6 mice, for which eGFPp is a foreign peptide, had on average 23,000 eGFPp:I-A^b-specific $CD44^{hi}$ $CD4^+$ T cells in their secondary lymphoid organs 14 days after immunization (Fig. 1a). Most of these cells were $Foxp3^-$ effector T cells, although a small subpopulation of $Foxp3^+$ T_{reg} cells was present (Fig. 1c). The $Foxp3^-$ population consisted of 10% $ROR\gamma t^+$ T_H17 cells, 22% T-bet^+ T_H1 cells, 30% Bcl-6^+ T_{FH} cells, and 35% could not be assigned to a known lineage (Fig. 1c).

The eGFP-, eYFP-, or CFP-transgenic mice generated a spectrum of eGFPp:I-A^b-specific $CD44^{hi}$ $CD4^+$ effector T cell numbers in secondary lymphoid organs following immunization (Fig. 1a). At one end, insulin 1 (*Ins1*)^{eGFP} mice produced the same number of cells as wild-type mice, indicating a complete lack of tolerance. At the other end, ubiquitin (*UBC*)^{eGFP} mice generated fewer than 100 eGFPp:I-A^b-specific $CD44^{hi}$ T cells, indicating a profound state of tolerance. The other 12 transgenic strains produced 200–10,000 eGFPp:I-A^b-specific $CD44^{hi}$ T cells (Fig. 1a).

The eGFPp:I-A^b-specific $CD44^{hi}$ T cells in the transgenic mice also displayed a range of phenotypes. T_{reg}, T_H1, T_{FH}, and T_H17 cells generated in each strain after priming with

eGFPp in CFA were analyzed using an unsupervised hierarchical clustering algorithm[17] to search for patterns of tolerance induction (Fig. 1d). Absolute cell numbers were used for this clustering to capture information about clonal proliferation and differentiation. This analysis revealed three major clusters. Cluster 1 was typified by *Ins1*^{eGFP} mice and was characterized by wild-type numbers of T_{FH}, T_H1, and T_H17 cells and relatively few T_{reg} cells (Fig. 1d,e). Cluster 2 was exemplified by *Ins2*^{eGFP} mice and contained low numbers of T_{FH}, T_H1, and T_H17 cells and relatively large numbers of T_{reg} cells (Fig. 1d,e). Cluster 3 was typified by *UBC*^{eGFP} mice and characterized by profound reduction of all subsets (Fig. 1d,e). These results suggest that three major mechanisms account for $CD4^+$ T cell tolerance to self-antigens with different patterns of expression.

Ignorance is the tolerance mechanism for Cluster 1

Cluster 1 contained wild-type mice and mice with patterns of very limited eGFP expression: *Ins1*^{eGFP} mice express eGFP exclusively in pancreatic beta cells[18, 19], whereas Forkhead box D1 (*Foxd1*)^{eGFP} mice express eGFP during kidney and eye development[20, 21]. Because *Ins1*^{eGFP} and *Foxd1*^{eGFP} mice responded to eGFPp immunization like mice that did not express eGFP, it is likely that their eGFPp:I-A^b-specific T cell repertoires never encountered this epitope and were in a naive state. We tested this hypothesis in *Ins1*^{eGFP} mice by enumerating eGFPp:I-A^b-specific $CD4^+$ T cells in unimmunized mice (Fig. 2a,b). Single cell suspensions of secondary lymphoid organs were stained with eGFPp:I-A^b tetramers labeled with allophycocyanin or phycoerythrin, then with anti-phycoerythrin and anti-allophycocyanin magnetic beads before magnetic enrichment. Cells were stained with the same tetramer labeled with two different fluorochromes to maximize the TCR specificity of the assay[16]. *Ins1*^{eGFP} mice contained an average of 19 eGFPp:I-A^b-specific $CD4^+$ T cells in secondary lymphoid organs, like wild-type mice (Fig. 2b). These populations also had similar frequencies of naive-phenotype ($CD44^{lo}$) cells (Fig. 2c). Together with the observation that *Ins1*^{eGFP} and wild-type mice mounted comparable responses following immunization, these results indicated that tolerance in Cluster 1 was due to ignorance.

Partial clonal deletion and T_{reg} induction shape Cluster 2

Cluster 2 was characterized by low numbers of effector cells and relatively large numbers of T_{reg} cells in mice primed with eGFPp. It consisted of several mice with tissue-restricted promoters that are also expressed sparsely in the thymus. *Ins2*^{eGFP} mice express eGFP fused to the C peptide of pro-insulin in pancreatic beta cells[22]. They also express eGFP in a small number of medullary thymic epithelial cells[19]. Forkhead box P3 (*Foxp3*)^{eGFP} mice express eGFP in developing T_{reg} cells in the thymus, whereas *CD207*^{eYFP} mice[23] express eYFP in epidermal Langerhans cells and perhaps thymic dendritic cells. Smooth muscle myosin heavy chain 11 (*Myh11*)^{eGFP} and zinc finger protein 423 (*Zfp423*)^{eGFP} mice are expected to express eGFP at moderate levels in medullary thymic epithelial cells[24]. Purkinje cell protein 2 (*Pcp2*)^{eGFP} mice, which express eGFP in cerebellar Purkinje neurons in the brain[25] were also in this cluster. *Ins2*^{eGFP} mice were selected for further analysis of the tolerance mechanisms operating in Cluster 2.

Evidence for intrathymic clonal deletion was sought by enumerating eGFPp:I-A^b-specific $CD4^+CD8^-$ thymocytes (Fig. 3). Wild-type mice contained an average of 16 eGFPp:I-A^b-

specific $CD4^+CD8^-$ thymocytes and 20 peripheral $CD4^+$ T cells, whereas *Ins2*^{eGFP} mice had an average of 10 and 13 such cells (Fig. 3a–d). These results indicated that about 30% of eGFPp:I-A^b-specific T cell clones were deleted in *Ins2*^{eGFP} mice. $Foxp3^+$ eGFPp:I-A^b-specific $CD4^+CD8^-$ thymocytes were detected in wild-type and *Ins2*^{eGFP} thymuses, although not in all mice due to the small size of this population. However, significantly more *Ins2*^{eGFP} thymuses (40%) contained eGFPp:I-A^b-specific $Foxp3^+$ $CD4^+CD8^-$ thymocytes than wild-type thymuses (Fig. 3e,f). Thus, T_{reg} cells were spared from deletion or even increased in the presence of this self-antigen.

The clones that were deleted in *Ins2*^{eGFP} mice might have had TCRs with the highest affinities for the eGFPp:I-A^b epitope. This possibility was addressed by measuring the mean fluorescence intensity of tetramer binding, which is a direct correlate of TCR affinity for peptide:MHCII[26]. Thymocytes could not be used for this purpose because they were too rare for an accurate measurement. The analysis was therefore performed on expanded populations of eGFPp:I-A^b-specific cells in immunized mice. No significant difference was found in the mean fluorescence intensity of eGFPp:I-A^b tetramer staining on cells from wild-type or *Ins2*^{eGFP} mice immunized with eGFPp in CFA. Because CFA forms a long-lasting depot at the injection site[27], persistent presentation of the eGFPp:I-A^b epitope may have given low affinity T cells an advantage thereby reducing the capacity to detect a subtle difference. The analysis was therefore repeated using an eGFP-expressing strain of attenuated (Δ*actA*Δ*inlB*) *Listeria monocytogenes* (Lm-eGFP) that causes a very transient infection[28]. Lm-eGFP-induced clonal proliferation of eGFPp:I-A^b-specific T cells was significantly impaired in *Ins2*^{eGFP} mice compared to wild-type mice (Fig. 4 a,b). Furthermore, the mean fluorescence intensity of eGFPp:I-A^b tetramer staining on cells from *Ins2*^{eGFP} mice was lower than that of cells from wild-type mice (Fig. 4c). These results indicate that some clones with TCRs with high affinity for the eGFPp:I-A^b epitope are deleted in *Ins2*^{eGFP} mice.

The fact that eGFP was likely expressed in the thymuses of *Ins2*^{eGFP} mice under the control of the transcriptional regulator Aire led to an investigation of whether tolerance occurred in this organ in an Aire-dependent fashion. This question was first addressed by transplanting wild-type or *Ins2*^{eGFP} thymuses into athymic B6-nude mice[29]. Eight-twelve weeks later, mice were primed subcutaneously with eGFPp in CFA. B6-nude recipients of wild-type thymus grafts generated large numbers of $CD44^{hi}$ eGFPp:I-A^b-specific $CD4^+$ T cells as seen in intact wild-type mice, whereas B6-nude mice that received *Ins2*^{eGFP} thymus grafts produced a much smaller population (Fig. 5a). B6-nude recipients of *Ins2*^{eGFP} thymus grafts produced higher numbers and frequencies of $CD44^{hi}$ eGFPp:I-A^b-specific T_{reg} cells than the recipients of wild-type thymus grafts (Fig. 5b,c). $Foxp3^-$ effector cell differentiation was also impaired in *Ins2*^{eGFP} thymus graft recipients (Fig. 5d). Thus, much of the tolerance observed in *Ins2*^{eGFP} mice was induced in the thymus.

The involvement of Aire was tested using *Ins2*^{eGFP}*Aire*$^{-/-}$ mice. These mice had comparable numbers of eGFPp:I-A^b-specific $CD4^+CD8^-$ thymocytes as wild-type and *Aire*$^{-/-}$ mice (Fig. 5e), demonstrating that clonal deletion in *Ins2*^{eGFP} mice was Aire-dependent. Furthermore, thymic T_{reg} cell numbers in *Ins2*^{eGFP}*Aire*$^{-/-}$ mice were similar to wild-type levels **(data not shown)** and clonal proliferation and differentiation of $Foxp3^-$

effector cells was very similar in *Ins2*^{eGFP}*Aire*$^{-/-}$ and *Aire*$^{-/-}$ mice following immunization (Fig. 5f–h). Therefore, much of the tolerance in *Ins2*^{eGFP} mice was induced in the thymus by an Aire-dependent mechanism. Total numbers of Foxp3^{+} T_{reg} cells, however, were still elevated in some immunized *Ins2*^{eGFP}*Aire*$^{-/-}$ mice compared to wild-type mice, suggesting that a non-Aire-dependent mechanism could play a role in this aspect of tolerance (Fig. 5g).

Overall, these studies indicate that tolerance in CD4^{+} T cell repertoires specific for self-epitopes expressed in a limited fashion in the thymus is associated with intrathymic deletion of some clones and impaired effector, but enhanced T_{reg} cell generation from the remaining clones.

Clonal deletion regulates self-antigens in Cluster 3

Cluster 3 was characterized by a profound clonal proliferation defect following immunization. This cluster contained mice that express eGFP under the control of non-Aire-regulated promoters in MHCII^{+} cells in the thymus. *UBC*^{eGFP} and beta actin (*ACTB*)^{eGFP} mice express eGFP in thymic dendritic cells, medullary thymic epithelial cells, and all other nucleated cells[30, 31]. CD11c (*Itgax*)^{eYFP} mice express eYFP in thymic dendritic cells[32], whereas choline acetyltransferase (*Chat*)^{eGFP} [33, 34], cadherin 1 (*Cdh1*)^{CFP} [35] and *Aire*^{eGFP} [36] mice express eGFP in medullary thymic epithelial cells. *UBC*^{eGFP} mice were chosen for further analysis as a representative of Cluster 3.

eGFPp:I-A^{b}-specific CD4^{+}CD8^{-} thymocytes were enumerated to determine whether intrathymic clonal deletion was responsible for the proliferation defect observed in *UBC*^{eGFP} mice (Fig. 6). Wild-type mice contained an average of 20 eGFPp:I-A^{b}-specific CD4^{+}CD8^{-} thymocytes, while *UBC*^{eGFP} mice had less than one. A few eGFPp:I-A^{b}-specific CD4^{+} T cells were, however, detected in the secondary lymphoid organs of *UBC*^{eGFP} mice (Fig. 6c,d). These results suggest that most eGFPp:I-A^{b}-specific CD4^{+}CD8^{-} thymocytes are deleted in the thymus, although a few escape and accumulate in the secondary lymphoid organs. The profound lack of proliferation following immunization indicated that these few cells were unresponsive. These results indicate that MHCII-bound peptides from proteins that are abundantly expressed in MHCII^{+} cells in the thymus induce a profound state of immune tolerance mediated in large part by intrathymic clonal deletion.

Thymic self-antigen expression correlates with tolerance

The specific mechanisms of tolerance associated with self-epitopes in Clusters 1–3 appeared to depend on self-antigen expression by MHCII^{+} cells in the thymus. To test this hypothesis, representatives from these clusters were examined for expression of eGFP and eYFP by EpCAM^{+} thymic epithelial cells and thymic dendritic cells (Supplementary Fig. 1). Thymuses from wild-type and *Ins1*^{eGFP} mice, members of Cluster 1, contained fewer than 10 I-A^{b+} eGFP^{+} or eYFP^{+} EpCAM^{+} epithelial cells or dendritic cells, consistent with the ignorant phenotype of eGFPp:I-A^{b}-specific CD4^{+} T cells in these mice (Fig. 7a–c). At the other end of the spectrum, *Itgax*^{eYFP} and *ACTB*^{eGFP} mice, members of Cluster 3, contained more than 300,000 I-A^{b+} eYFP^{+} or eGFP^{+} dendritic cells and EpCAM^{+} epithelial cells in their thymuses, likely accounting for the substantial clonal deletion observed in these mice (Fig. 7a–c). Finally, *Ins2*^{eGFP}, *Pcp2*^{eGFP}, and *CD207*^{eYFP} thymuses contained several

hundred I-A^{b+} $eGFP^+$ or $eYFP^+$ $EpCAM^+$ epithelial cells, and *CD207*^{eYFP} thymuses also contained ~3,000 I-A^{b+} $eYFP^+$ dendritic cells (Fig. 7a–c). A significant inverse correlation was observed between the number of $eGFP^+$ or $eYFP^+$ thymic antigen-presenting cells and the number of eGFPp:I-A^b-specific $CD4^+$ T cells present 14 days after immunization (Fig. 7d). These results are consistent with the hypothesis that the number of $MHCII^+$ thymic antigen-presenting cells expressing a particular self-antigen determines the responsiveness of the corresponding $CD4^+$ T cell population.

Tolerance to true self-antigens occurs by these mechanisms

Information from the eGFP system was then used to identify the tolerance mechanisms for $CD4^+$ T cell repertoires for 6 genuine self-peptide:I-A^b epitopes. B6 mice were immunized with the self-peptides or foreign peptides as controls, and the compositions of the resulting $Foxp3^-$ effector and $Foxp3^+$ T_{reg} cell populations were determined. The percentages of T_{FH}, T_H1, T_H17, and T_{reg} cells were analyzed using an unsupervised hierarchical clustering algorithm to determine if the responses to the self-peptides aligned with the clusters defined in the eGFP system. Percentages of cells in each subset, rather than absolute numbers, were used for this comparison because the sizes of the pre-immunization repertoires for the natural epitopes were unknown. The use of absolute numbers of cells in each subset would have been problematic for epitopes with populations that had the same differentiation potential but simply varied in size.

Peptides from the constant region of IgM (IgMHp), which is very abundant in the blood, or ATP-binding cassette sub-family G, member 1 (ABCG1p), which is highly expressed in thymic dendritic cells and medullary thymic epithelial cells[24], elicited fewer than 200 $CD44^{hi}$ cells that bound the relevant peptide:I-A^b tetramers (Fig. 8a). These peptides elicited too few $CD44^{hi}$ cells to accurately determine the percentages of each subset and thus were not analyzed by the clustering algorithm. The minimal responses to these self-epitopes, however, indicated that these $CD4^+$ T cell repertoires underwent extensive intrathymic clonal deletion as in the eGFP transgenic mice in Cluster 3.

The unsupervised hierarchical clustering analysis produced 2 clusters. The first (‘foreign’) cluster contained responses to foreign peptides from listeriolysin O protein of *Listeria monocytogenes* (LLOp)[37, 38], calnexin from *Blastomyces dermatitidis* (CLGN(BD)p), and a model peptide called 2W[39], as well as the Cluster 1 (Fig. 1d) responses to eGFPp in wild-type, *Ins1*^{eGFP}, and *Foxd1*^{eGFP} mice (Fig. 8b). The second (‘self’) cluster consisted of responses to the eGFP epitope in the eGFP transgenic mice that comprised Cluster 2 (Fig. 1d).

A peptide from junctophilin 2 (JPH2p), which is expressed exclusively in skeletal muscle and the heart[40], elicited 5,000 $CD44^{hi}$ cells that bound the relevant peptide:I-A^b tetramer (Fig. 8a). This population produced a T_{reg} and effector cell composition similar to that of populations specific for foreign peptides, as evidenced by its assignment to the ‘foreign’ cluster (Fig. 8b). These results indicate that $CD4^+$ T cell tolerance to the junctophilin 2 epitope in B6 mice is maintained by ignorance.

Peptides from myelin oligodendrocyte glycoprotein (MOG) and proteolipid protein (PLP), which are expressed in the nervous system, and protein disulfide associated isomerase 2 (PDIA2), which is expressed in the pancreas and digestive tract[41], elicited 1,000–10,000 peptide:I-A^b-specific $CD44^{hi}$ cells (Fig. 8a). These populations contained reduced $Foxp3^-$ effector and increased T_{reg} cell frequencies compared to populations specific for non-mouse peptides (Fig. 8b). The responses to these self-epitopes were placed in the 'self' cluster, which also contained responses to the eGFP epitope in the eGFP transgenic mice that comprised Cluster 2 in Figure 1d. Thus, tolerance to these endogenously expressed peptides resembled that associated with limited thymic eGFP expression.

DISCUSSION

Here we demonstrate that tolerance in the normally diverse $CD4^+$ T cell repertoire is attributed to one of three mechanisms depending on the expression pattern of the self-epitope.

A profound state of tolerance existed in $CD4^+$ T cell repertoires specific for epitopes from proteins that are easily accessed or expressed by many $MHCII^+$ cells in the thymus. This tolerance manifested as nearly complete deletion of self-epitope-specific T cells in the thymus, which likely resulted from abundant self-epitope display on $MHCII^+$ thymic dendritic cells and/or medullary thymic epithelial cells. Although substantial clonal deletion was reported for human and murine T cells specific for self-epitopes from the Y-chromosome or driven by the *ACTB* promoter[4, 5, 15], it was not as extensive as that observed here for an epitope expressed from the *UBC* promoter. This promoter may have led to an extraordinarily large number of self-epitopes on thymic antigen-presenting cells, causing deletion of nearly all self-epitope-specific T cells. Alternatively, deletion within the small eGFPp:I-A^b-specific $CD4^+$ T cell repertoire might have been more efficient because of limited inter-clonal competition.

A state of immunological ignorance existed within $CD4^+$ T cell repertoires specific for epitopes from non-Aire-regulated proteins that are expressed exclusively outside of the thymus. In addition, these epitopes are probably not displayed in secondary lymphoid organs because their parent proteins are cytosolic and expressed by cells that do not turn over in a way that allows local dendritic cells to produce the epitopes or access draining lymph nodes. The complete lack of presentation of these self-epitopes dictates that corresponding $CD4^+$ T cells exist in a naive and fully responsive state of ignorance. Self-epitopes in this cluster are essentially foreign to the relevant T cell repertoires.

A complex form of tolerance controlled $CD4^+$ T cell repertoires specific for epitopes from proteins with tissue-restricted patterns of expression, but that are also expressed by small numbers of $MHCII^+$ thymic antigen-presenting cells. Analysis of the *Ins2*^{eGFP} member of this group revealed that tolerance was associated with intrathymic deletion of ~30% of the epitope-specific clones. Partial clonal deletion was also observed in studies of a polyclonal $CD8^+$ T cell population specific for a tissue-restricted epitope[11]. In our studies, the deleted clones had TCRs with the highest affinities for the eGFPp:I-A^b ligand. Thymocytes with high affinity TCRs might be especially sensitive to deletion because they can garner

sufficient signal from single encounters with rare thymic antigen-presenting cells. In contrast, deletion of thymocytes with lower affinity TCRs may require numerous encounters[42, 43], which are unlikely to occur when relevant thymic antigen-presenting cells are rare, as in Cluster 2.

The partial deletion of the epitope-specific polyclonal population studied in *Ins2*^{eGFP} mice depended on Aire, indicating involvement of medullary thymic epithelial cells. Furthermore, we found that expression of eGFP from the *Ins2, Pcp2,* and *CD207* loci occurred in only a small number of thymic epithelial cells and dendritic cells, likely allowing eGFPp:I-A^b-specific T cells with lower affinity TCRs to escape deletion. In agreement with this possibility, eGFPp:I-A^b-specific T cells were nearly completely deleted in *Aire*^{eGFP} mice, which express eGFP in all medullary thymic epithelial cells[36]. Although medullary thymic epithelial cells were a likely source of eGFP in these models, antigen transfer to neighboring dendritic cells could have mediated deletion[44].

The non-deleted T cells specific for Cluster 2 epitopes generated Foxp3$^-$ effector T cells less well than corresponding wild-type T cells. This defect extended to T_{FH} cells but was particularly striking for T_H1 and T_H17 cells. Other work has shown that T_H1 clones tend to have higher affinity TCRs than T_{FH} cells[45]. Thus, it is possible that the lower affinity TCRs found on epitope-specific T cells in this cluster were incapable of generating enough signals to form T_H1 and T_H17 cells. Alternatively, these cells might have been induced into a partially anergic state due to persistent self-epitope recognition in a non-inflammatory environment as suggested by previous TCR transgenic studies[46, 47, 48]. If so, the thymic transplant experiments presented here suggest that this anergy induction occurs mainly in the thymus.

Enhanced T_{reg} cell proliferation after immunization was another component of tolerance to the epitopes in Cluster 2. One explanation for this feature is that the pre-immunization repertoires of T cells specific for these epitopes are enriched for thymus-derived T_{reg} cells, which might occur when cells are shunted into the T_{reg} cell lineage following moderately high affinity self-epitope recognition in the thymus[49]. The observation that T_{reg} cells were detected more frequently in the pre-immunization eGFPp:I-A^b-specific population in *Ins2*^{eGFP} mice than in wild-type mice is consistent with this possibility. This is only a tentative conclusion however, because the eGFPp:I-A^b-specific populations were very small in both situations. It is also possible that Foxp3$^-$ cells in the eGFPp:I-A^b-specific population had enhanced potential to differentiate into induced T_{reg} cells after immunization. In any case, our results suggest that T_{reg} cells are especially important for tolerance to epitopes from tissue-restricted antigens that also exhibit limited thymic expression.

The mechanisms of tolerance identified for the epitopes studied here all appeared to be induced in the thymus. It is possible that other epitopes are tolerated by mechanisms that operate in the secondary lymphoid organs, for example, epitopes from paternal fetal proteins that appear in pregnant females. Peripheral deletion and anergy appear to be the tolerance mechanisms for these antigens[50].

ONLINE METHODS

Mice

Four- to 8-week old C57BL/6 (B6), B6.Cg-*Foxn1*^{nu}/J (B6-nude), B6.PL-*Thy1*^{a}/CyJ (CD90.1), C57BL/6-Tg(UBC-GFP)30Scha/J (*UBC*^{eGFP}), B6.Cg-Tg(Ins1-EGFP)1Hara/J (*Ins1*^{eGFP}), B6.Cg-Tg(RP23-268L19-EGFP)2Mik/J (*Chat*^{eGFP}), B6;FVB-Tg(Zfp423-EGFP)7Brsp/J (*Zfp423*^{eGFP})[51], B6.Cg-Tg(Myh11-cre,-EGFP)2Mik/J (*Myh11*^{eGFP})[52], B6.129P2(Cg)-*Cdh1*^{tm1Cle}/J (*Cdh1*^{eGFP}), B6;129S4-*Foxd1*$^{tm1(GFP/cre)Amc}$/J (*Foxd1*^{eGFP}), and C57BL/6-Tg(CAG-EGFP)131Osb/LeySopJ (*ACTB*^{eGFP}) mice were purchased from the Jackson Laboratory or the National Cancer Institute Mouse Repository (Frederick, MD, USA). Mice were used at 6–12 weeks of age. (*Ins2*^{eGFP} x B6), (*Ins2*^{eGFP} x CD90.1), (*Ins1*^{eGFP} x B6), (*Ins2*^{eGFP}*Aire*$^{+/-}$ x *Aire*$^{+/-}$), STOCK Tg(Pcp2-EGFP)BT153Gsat/Mmmh, (backcrossed >8 generations onto the B6 background) (*Pcp2*^{eGFP}), B6.Cg-Tg(Itgax-Venus)1Mnz/J (*Itgax*^{eYFP}), *CD207*^{cre} x B6.129X1-Gt(ROSA)26Sortm1(EYFP)Cos/J (*CD207*^{eYFP})[23], and *Foxp3*^{eGFP} mice[53] were bred and housed under specific-pathogen free conditions as per the guidelines of the University of Minnesota Institutional Animal Care and Use Committee and the National Institutes of Health. *Aire*^{eGFP} mice[36] were bred and housed under specific-pathogen free conditions in accordance with the National Institutes of Health and American Association of Laboratory Animal Care standards, and with the animal care and use regulations of the University of California, San Francisco. Analysis of thymus cell numbers was carried out between 3 and 5 weeks of age.

Immunizations

Mice were injected subcutaneously with 100 μl (split over 2 sites) of CFA (Sigma-Aldrich) emulsion containing 100 μg of peptide (GenScript) in DPBS (Life Technologies). Mice were immunized with the specific peptides contained in the tetramers below with the following exceptions: MOGp (GWYRSPFSRVVHL) and CLGN(BD)p (LVVKNPAAHHAI).

Infections

The Δ*actA*Δ*inlB* strain of Lm-eGFP (PL1113) was provided by Peter Lauer. Briefly, the eGFP construct (hyperSPO1 promoter-eGFP)[54] was cloned into the pPL1 vector[55] and integrated at the *comK* locus in the *actA*-*inlB*-double mutant[56]. Mice were injected i.v. with 1×10^{7} Lm-eGFP bacteria and analyzed 6–7 days post-infection.

Tetramers

Biotin-labeled I-A^{b} monomers containing the eGFPp (HDFFKSAMPEGYVQE), 2W (EAWGALANWAVDSA), LLOp (NEKYAQAYPNVS), CLGN(BD)p (LVVKNPAAHHAIS), JPH2p (VYTWPSGNTFE), MOGp (GWYRSPFSRVV), PLPp (CLVGAPFASLVA), IgMHp (EKYVTSAPMPEPGAPG)[57], I-A^{b}-binding-stabilized variant of ABCG1p (YYMTPQPSDVV), or PDIA2p (EYSKAAALLAA) peptides covalently linked to the I-A^{b} beta chain were grown in *Drosophila melanogaster* S2 cells also expressing the I-A^{b} alpha chain, purified and combined with streptavidin (SA)-phycoerythrin (PE) or (SA)-allophycocyanin (APC) (Prozyme, San Leandro, CA, USA) to produce fluorescently labeled I-A^{b} tetramers as previously described [16, 37, 58].

Cell enrichment and flow cytometry

Single cell suspensions were prepared from pooled murine spleens and lymph nodes (axillary, brachial, inguinal, cervical, mesenteric, pancreatic, and para-aortic) or thymuses by mechanical disruption. Cells were stained for 1 hour at room temperature with allophycocyanin-conjugated tetramers. In some experiments cells were also stained with anti-CXCR5 (2G8, BD) antibody or phycoerythrin-conjugated tetramers. Tetramer-binding cells were enriched on magnetized columns as described previously[58]. For thymic epithelial cell and dendritic cell analysis, thymuses were harvested and enzymatically digested as previously described[59]. Single cell suspensions were stained with a biotinylated antibody to CD11c (HL3, BD) and an allophycocyanin-labeled antibody to EpCAM (G8.8, Biolegend). Cells were incubated with anti-biotin and anti-allophycocyanin cocktails and magnetic beads (StemCell Technologies). Cells were enriched using the EasySep system according to the manufacturer's instructions (StemCell Technologies).

Antibodies

Tetramer-enriched samples were stained for surface markers for 30 minutes on ice using antibodies to: CD4 (GK1.5, BD), CD8 (53–6.7, BD), CD90.1 (HIS51), CD90.2 (53–2.1, 30-H12), CD3e (145-2C11, BD), CD11b (M1/70), CD11c (N418), F4/80 (BM8), CD44 (IM7, BD), CD45.1 (A20, Biolegend), CD45.2 (104), B220 (RA3–6B2), and/or PD1 (J43). Cellular viability was confirmed using GhostDye Red 780 (Tonbo Biosciences). For transcription factor expression analysis, stained cells were fixed and permeablized using the Foxp3/Transcription Factor Staining Buffer Set (eBioscience) according to the manufacturer's instructions. Cells were stained overnight at 4°C with antibodies to T-bet (4B10, Biolegend), Foxp3 (FJK-16s), RORγt (Q31-378, BD), and Bcl-6 (K112-91, BD). For thymic dendritic cell and thymic epithelial cell analyses cells, following enrichment cells were stained with antibodies to CD11c (N418), CD19 (6D5, Biolegend), I-A/I-E (M5/114.15.2, Biolegend), CD8 (53–6.7, BD), CD90.2 (53–2.1, 30-H12), CD11b (M1/70), and CD45.2 (104, BD). Antibodies were purchased from eBioscience unless otherwise indicated. Cells were analyzed by flow cytometry on a Fortessa (BD). Data were analyzed using FlowJo software (TreeStar).

Thymus transplants

Thymus transplants were performed as previously described [60]. Briefly, thymus lobes were harvested from prenatal (post-conception day 18) pups generated by crossing *Ins2*^{eGFP} and CD90.1^{+} B6 mice. An incision was made on the left abdomen of anesthetized 4–6 week old female B6-nude to expose the kidney and the donor thymic lobes were grafted beneath the kidney capsule. The muscle layer was sutured and the skin was closed using surgical clips. Thymic engraftment was assessed 6 weeks after transplantation by examining peripheral blood for the presence of mature αβ T cells by flow cytometry. Donor genotypes were determined post-transplantation.

Statistics

Two-tailed, unpaired Student's t tests, one-way ANOVA, Chi-square test, and linear regression were performed using Prism (Graphpad) software.

Hierarchical Clustering

Unsupervised hierarchical clustering and heatmap generation was carried out using the 'HierarchicalClustering' and 'HierarchicalClusteringViewer' modules from GenePattern (http://genepattern.broadinstitute.org)[17, 61, 62].

Supplementary Material

Refer to Web version on PubMed Central for supplementary material.

Acknowledgments

We thank Dan Mueller for reviewing the manuscript and Jennifer Walter and Orion Rainwater for technical assistance. We thank Peter Lauer (and Aduro Biotech) for providing the Lm-eGFP strain: PL1113. Supported by grants from the US National Institutes of Health (P01 AI35296 to M.K.J. and K.A.H.; F32 AI114050 to D.M.; T32 GM008244 and F30 DK093242 to R.W.N; T32 AI07313 to J.L.L; K99 AI114884 to Y.J.L), the Wallin Neuroscience Discovery Fund (to H.T.O. and M.K.J.), and the Juvenile Diabetes Research Foundation Grant 2-2011-662 (to B.T.F.).

References

1. Xing Y, Hogquist KA. T-cell tolerance: central and peripheral. Cold Spring Harb Perspect Biol. 2012; 4
2. Wing K, Sakaguchi S. Regulatory T cells exert checks and balances on self tolerance and autoimmunity. Nat Immunol. 2010; 11:7–13. [PubMed: 20016504]
3. Semana G, Gausling R, Jackson RA, Hafler DA. T cell autoreactivity to proinsulin epitopes in diabetic patients and healthy subjects. J Autoimmun. 1999; 12:259–267. [PubMed: 10330297]
4. Moon JJ, et al. Quantitative impact of thymic selection on Foxp3+ and Foxp3- subsets of self-peptide/MHC class II-specific CD4+ T cells. Proc Natl Acad Sci USA. 2011; 108:14602–14607. [PubMed: 21873213]
5. Yu W, et al. Clonal deletion prunes but does not eliminate self-specific alphabeta CD8(+) T lymphocytes. Immunity. 2015; 42:929–941. [PubMed: 25992863]
6. Maeda Y, et al. Detection of self-reactive CD8(+) T cells with an anergic phenotype in healthy individuals. Science. 2014; 346:1536–1540. [PubMed: 25525252]
7. Ohashi PS, et al. Ablation of "tolerance" and induction of diabetes by virus infection in viral antigen transgenic mice. Cell. 1991; 65:305–317. [PubMed: 1901764]
8. Oldstone MB, Nerenberg M, Southern P, Price J, Lewicki H. Virus infection triggers insulin-dependent diabetes mellitus in a transgenic model: role of anti-self (virus) immune response. Cell. 1991; 65:319–331. [PubMed: 1901765]
9. Jenkins MK, Schwartz RH. Antigen presentation by chemically modified splenocytes induces antigen-specific T cell unresponsiveness in vitro and in vivo. J Exp Med. 1987; 165:302–319. [PubMed: 3029267]
10. Akkaraju S, et al. A range of CD4 T cell tolerance: partial inactivation to organ-specific antigen allows nondestructive thyroiditis or insulitis. Immunity. 1997; 7:255–271. [PubMed: 9285410]
11. Zehn D, Bevan MJ. T cells with low avidity for a tissue-restricted antigen routinely evade central and peripheral tolerance and cause autoimmunity. Immunity. 2006; 25:261–270. [PubMed: 16879996]
12. Hataye J, Moon JJ, Khoruts A, Reilly C, Jenkins MK. Naive and memory CD4+ T cell survival controlled by clonal abundance. Science. 2006; 312:114–116. [PubMed: 16513943]
13. Marzo AL, et al. Initial T cell frequency dictates memory CD8+ T cell lineage commitment. Nat Immunol. 2005; 6:793–799. [PubMed: 16025119]
14. Bautista JL, et al. Intraclonal competition limits the fate determination of regulatory T cells in the thymus. Nat Immunol. 2009; 10:610–617. [PubMed: 19430476]

15. Bouneaud C, Kourilsky P, Bousso P. Impact of negative selection on the T cell repertoire reactive to a self-peptide: a large fraction of T cell clones escapes clonal deletion. Immunity. 2000; 13:829–840. [PubMed: 11163198]
16. Nelson RW, et al. T cell receptor cross-reactivity between similar foreign and self peptides influences naive cell population size and autoimmunity. Immunity. 2015; 42:95–107. [PubMed: 25601203]
17. Reich M, et al. GenePattern 2.0. Nat Genet. 2006; 38:500–501. [PubMed: 16642009]
18. Hara M, et al. Transgenic mice with green fluorescent protein-labeled pancreatic beta -cells. Am J Physiol Endocrinol Metab. 2003; 284:E177–183. [PubMed: 12388130]
19. Anderson MS, et al. Projection of an immunological self shadow within the thymus by the aire protein. Science. 2002; 298:1395–1401. [PubMed: 12376594]
20. Carreres MI, et al. Transcription factor Foxd1 is required for the specification of the temporal retina in mammals. J Neurosci. 2011; 31:5673–5681. [PubMed: 21490208]
21. Kobayashi A, et al. Identification of a multipotent self-renewing stromal progenitor population during mammalian kidney organogenesis. Stem Cell Reports. 2014; 3:650–662. [PubMed: 25358792]
22. Ben-Yehudah A, et al. Specific dynamic and noninvasive labeling of pancreatic beta cells in reporter mice. Genesis. 2005; 43:166–174. [PubMed: 16283623]
23. Kaplan DH, et al. Autocrine/paracrine TGFbeta1 is required for the development of epidermal Langerhans cells. J Exp Med. 2007; 204:2545–2552. [PubMed: 17938236]
24. Heng TS, Painter MW. Immunological Genome Project C. The Immunological Genome Project: networks of gene expression in immune cells. Nat Immunol. 2008; 9:1091–1094. [PubMed: 18800157]
25. Gong S, et al. A gene expression atlas of the central nervous system based on bacterial artificial chromosomes. Nature. 2003; 425:917–925. [PubMed: 14586460]
26. Crawford F, Kozono H, White J, Marrack P, Kappler J. Detection of antigen-specific T cells with multivalent soluble class II MHC covalent peptide complexes. Immunity. 1998; 8:675–682. [PubMed: 9655481]
27. Warren HS, Vogel FR, Chedid LA. Current status of immunological adjuvants. Annu Rev Immunol. 1986; 4:369–388. [PubMed: 2871847]
28. Portnoy DA, Auerbuch V, Glomski IJ. The cell biology of Listeria monocytogenes infection: the intersection of bacterial pathogenesis and cell-mediated immunity. J Cell Biol. 2002; 158:409–414. [PubMed: 12163465]
29. Cordier AC, Haumont SM. Development of thymus, parathyroids, and ultimo-branchial bodies in NMRI and nude mice. Am J Anat. 1980; 157:227–263. [PubMed: 7405870]
30. Schaefer BC, Schaefer ML, Kappler JW, Marrack P, Kedl RM. Observation of antigen-dependent CD8+ T-cell/dendritic cell interactions in vivo. Cell Immunol. 2001; 214:110–122. [PubMed: 12088410]
31. Okabe M, Ikawa M, Kominami K, Nakanishi T, Nishimune Y. 'Green mice' as a source of ubiquitous green cells. FEBS Lett. 1997; 407:313–319. [PubMed: 9175875]
32. Lindquist RL, et al. Visualizing dendritic cell networks in vivo. Nat Immunol. 2004; 5:1243–1250. [PubMed: 15543150]
33. Panneck AR, et al. Cholinergic epithelial cell with chemosensory traits in murine thymic medulla. Cell Tissue Res. 2014; 358:737–748. [PubMed: 25300645]
34. Tallini YN, et al. BAC transgenic mice express enhanced green fluorescent protein in central and peripheral cholinergic neurons. Physiol Genomics. 2006; 27:391–397. [PubMed: 16940431]
35. Snippert HJ, et al. Intestinal crypt homeostasis results from neutral competition between symmetrically dividing Lgr5 stem cells. Cell. 2010; 143:134–144. [PubMed: 20887898]
36. Gardner JM, et al. Deletional tolerance mediated by extrathymic Aire-expressing cells. Science. 2008; 321:843–847. [PubMed: 18687966]
37. Pepper M, Pagan AJ, Igyarto BZ, Taylor JJ, Jenkins MK. Opposing signals from the Bcl6 transcription factor and the interleukin-2 receptor generate T helper 1 central and effector memory cells. Immunity. 2011; 35:583–595. [PubMed: 22018468]

38. Geginat G, Schenk S, Skoberne M, Goebel W, Hof H. A novel approach of direct ex vivo epitope mapping identifies dominant and subdominant CD4 and CD8 T cell epitopes from Listeria monocytogenes. J Immunol. 2001; 166:1877–1884. [PubMed: 11160235]
39. Rees W, et al. An inverse relationship between T cell receptor affinity and antigen dose during CD4(+) T cell responses in vivo and in vitro. Proc Natl Acad Sci USA. 1999; 96:9781–9786. [PubMed: 10449771]
40. Takeshima H, Komazaki S, Nishi M, Iino M, Kangawa K. Junctophilins: a novel family of junctional membrane complex proteins. Mol Cell. 2000; 6:11–22. [PubMed: 10949023]
41. Fu XM, Dai X, Ding J, Zhu BT. Pancreas-specific protein disulfide isomerase has a cell type-specific expression in various mouse tissues and is absent in human pancreatic adenocarcinoma cells: implications for its functions. J Mol Histol. 2009; 40:189–199. [PubMed: 19821078]
42. Rosette C, et al. The impact of duration versus extent of TCR occupancy on T cell activation: a revision of the kinetic proofreading model. Immunity. 2001; 15:59–70. [PubMed: 11485738]
43. Au-Yeung BB, et al. A sharp T-cell antigen receptor signaling threshold for T-cell proliferation. Proc Natl Acad Sci USA. 2014; 111:E3679–3688. [PubMed: 25136127]
44. Klein L, Kyewski B, Allen PM, Hogquist KA. Positive and negative selection of the T cell repertoire: what thymocytes see (and don't see). Nat Rev Immunol. 2014; 14:377–391. [PubMed: 24830344]
45. Tubo NJ, et al. Single naive CD4+ T cells from a diverse repertoire produce different effector cell types during infection. Cell. 2013; 153:785–796. [PubMed: 23663778]
46. Apostolou I, Sarukhan A, Klein L, von Boehmer H. Origin of regulatory T cells with known specificity for antigen. Nat Immunol. 2002; 3:756–763. [PubMed: 12089509]
47. Tanchot C, Barber DL, Chiodetti L, Schwartz RH. Adaptive tolerance of CD4+ T cells in vivo: multiple thresholds in response to a constant level of antigen presentation. J Immunol. 2001; 167:2030–2039. [PubMed: 11489985]
48. Kearney ER, Pape KA, Loh DY, Jenkins MK. Visualization of peptide-specific T cell immunity and peripheral tolerance induction in vivo. Immunity. 1994; 1:327–339. [PubMed: 7889419]
49. Lee HM, Bautista JL, Scott-Browne J, Mohan JF, Hsieh CS. A broad range of self-reactivity drives thymic regulatory T cell selection to limit responses to self. Immunity. 2012; 37:475–486. [PubMed: 22921379]
50. PrabhuDas M, et al. Immune mechanisms at the maternal-fetal interface: perspectives and challenges. Nat Immunol. 2015; 16:328–334. [PubMed: 25789673]
51. Gupta RK, et al. Zfp423 expression identifies committed preadipocytes and localizes to adipose endothelial and perivascular cells. Cell Metab. 2012; 15:230–239. [PubMed: 22326224]
52. Xin HB, Deng KY, Rishniw M, Ji G, Kotlikoff MI. Smooth muscle expression of Cre recombinase and eGFP in transgenic mice. Physiol Genomics. 2002; 10:211–215. [PubMed: 12209023]
53. Fontenot JD, et al. Regulatory T cell lineage specification by the forkhead transcription factor foxp3. Immunity. 2005; 22:329–341. [PubMed: 15780990]
54. Shen A, Higgins DE. The 5′ untranslated region-mediated enhancement of intracellular listeriolysin O production is required for Listeria monocytogenes pathogenicity. Mol Microbiol. 2005; 57:1460–1473. [PubMed: 16102013]
55. Lauer P, Chow MY, Loessner MJ, Portnoy DA, Calendar R. Construction, characterization, and use of two Listeria monocytogenes site-specific phage integration vectors. J Bacteriol. 2002; 184:4177–4186. [PubMed: 12107135]
56. Brockstedt DG, et al. Listeria-based cancer vaccines that segregate immunogenicity from toxicity. Proc Natl Acad Sci USA. 2004; 101:13832–13837. [PubMed: 15365184]
57. Chu HH, Moon JJ, Kruse AC, Pepper M, Jenkins MK. Negative selection and peptide chemistry determine the size of naive foreign peptide-MHC class II-specific CD4+ T cell populations. J Immunol. 2010; 185:4705–4713. [PubMed: 20861357]
58. Moon JJ, et al. Naive CD4(+) T cell frequency varies for different epitopes and predicts repertoire diversity and response magnitude. Immunity. 2007; 27:203–213. [PubMed: 17707129]
59. Malhotra D, et al. Transcriptional profiling of stroma from inflamed and resting lymph nodes defines immunological hallmarks. Nat Immunol. 2012; 13:499–510. [PubMed: 22466668]

60. Berzins SP, Boyd RL, Miller JF. The role of the thymus and recent thymic migrants in the maintenance of the adult peripheral lymphocyte pool. J Exp Med. 1998; 187:1839–1848. [PubMed: 9607924]

61. de Hoon MJ, Imoto S, Nolan J, Miyano S. Open source clustering software. Bioinformatics. 2004; 20:1453–1454. [PubMed: 14871861]

62. Eisen MB, Spellman PT, Brown PO, Botstein D. Cluster analysis and display of genome-wide expression patterns. Proc Natl Acad Sci USA. 1998; 95:14863–14868. [PubMed: 9843981]

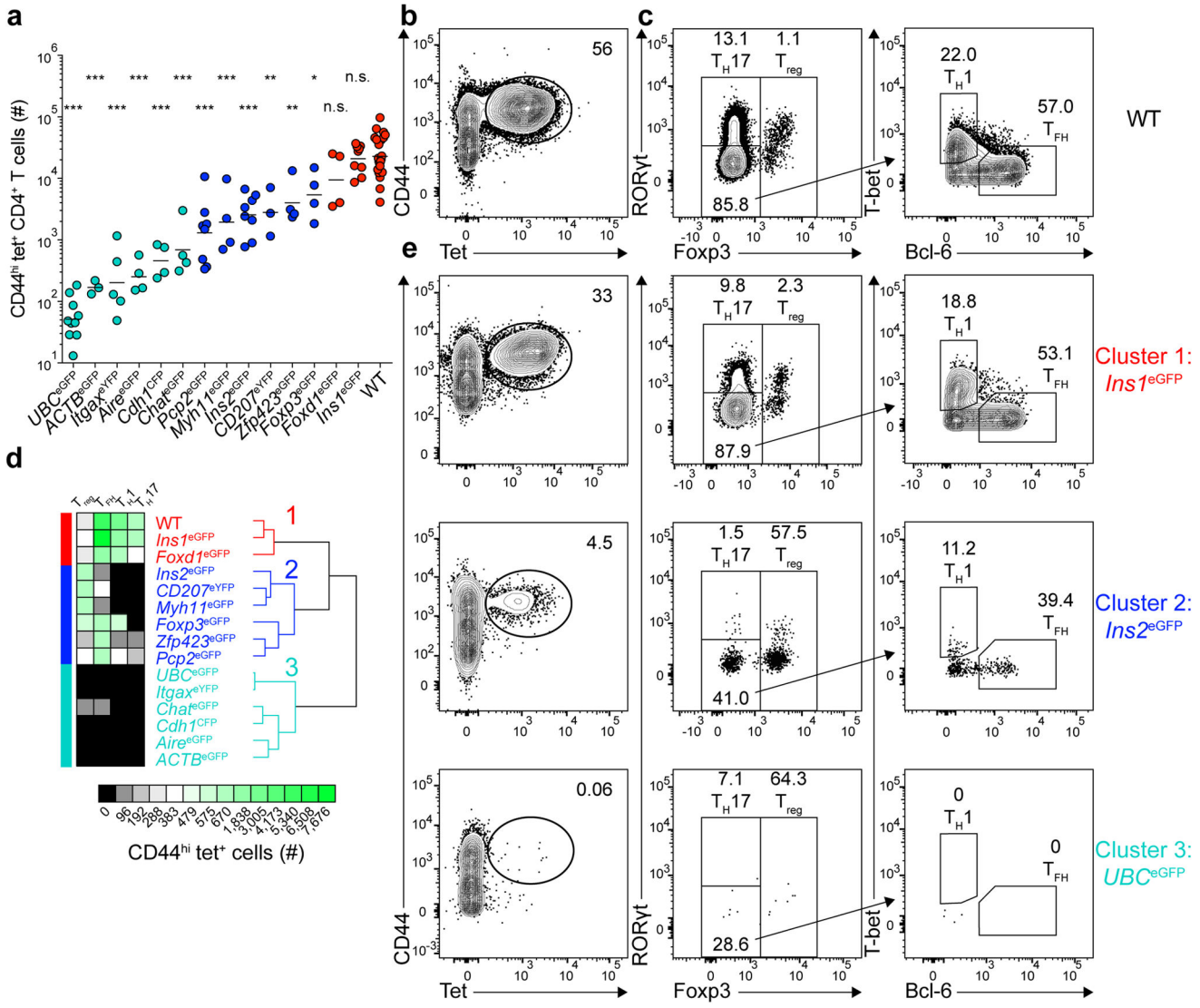

Figure 1. Three major patterns of tolerance to self-antigens

(a) Total number of CD44^{hi} tet^{+} (eGFPp:I-A^{b}-tetramer-binding) CD4^{+} T cells from pooled secondary lymphoid organs of mice 13–14 days after immunization with 100 μg of eGFPp emulsified in CFA. Horizontal bars indicate geometric mean values. Depicted results were pooled from 12 independent experiments, n=3–23 total mice per group. Circles represent individual mice and are colored according to the clusters identified in (d). (* P<0.05, ** P<0.005, *** P<0.0001, n.s. = not significant by one-way ANOVA of $\log_{10}$ transformed data relative to wild-type (WT) B6 mice).

(b) Contour plot showing CD44 and tetramer staining from tetramer-enriched CD4^{+} T cells from pooled secondary lymphoid organs of WT mice primed 14 days earlier with eGFPp in CFA. CD4^{+}CD44^{hi} tet^{+} cells are identified in the elliptical gate.

(c) Plots depicting transcription factor expression in the CD4^{+}CD44^{hi} tet^{+} cells identified in (b). Left, Foxp3 and RORγt expression by tet^{+} cells. Right, T-bet and Bcl-6 expression by Foxp3^{-}RORγt^{-} tet^{+} cells.

(d) Unsupervised hierarchical clustering of $CD4^+CD44^{hi}$ tet^+ T cells (geometric mean cell numbers and phenotypes) in the 15 indicated mouse strains using the HierarchicalClustering module from GenePattern. Three major clusters are indicated.

(e) Plots showing CD44 and tetramer staining of tetramer-enriched $CD4^+$ T cells from pooled secondary lymphoid organs of three different eGFP expressing mouse strains that are representative examples of Clusters 1–3, identified in (d) (left panel) and transcription factor expression by the $CD4^+CD44^{hi}$ tet^+ cells identified in the elliptical gates in the left panels. Numbers on each plot in (b–c) and (e) indicate the percent of cells in each gate.

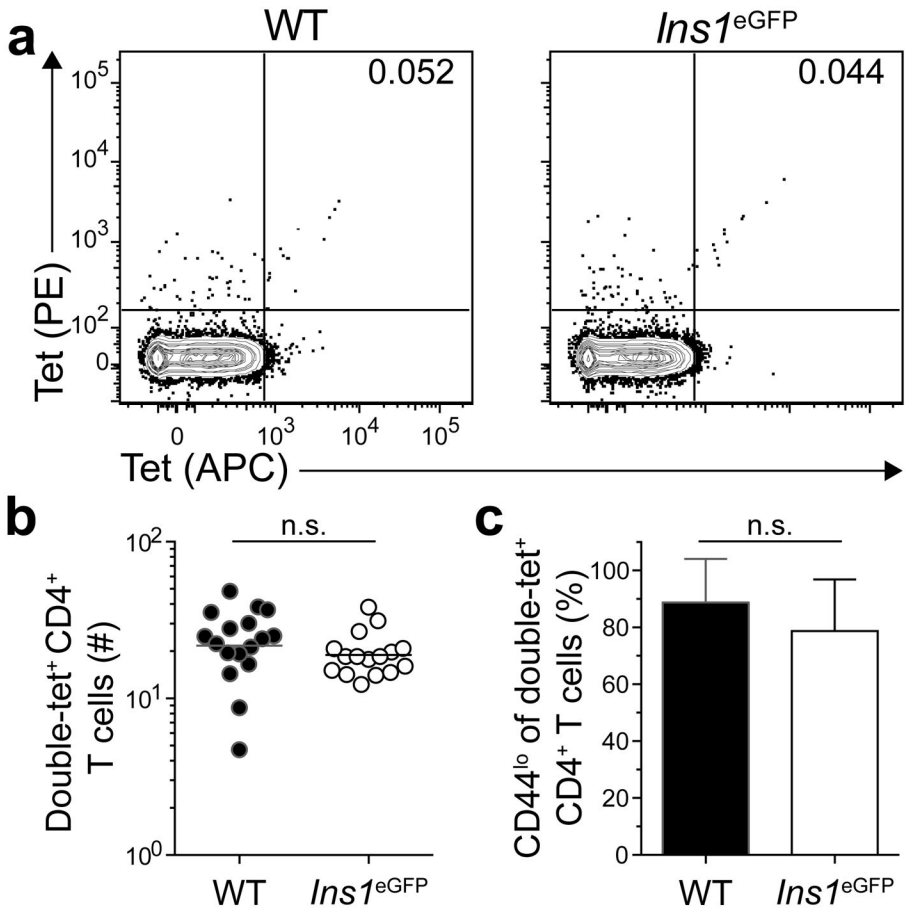

Figure 2. ***Ins1*^{eGFP} mice ignore the eGFPp:I-A^{b} epitope**

(a) Contour plots of eGFPp:I-A^{b}-streptavidin-phycoerythrin (tet-PE) versus eGFPp:I-A^{b}-streptavidin-allophycocyanin (tet-APC) staining of tetramer-enriched CD4^{+} T cells from pooled spleens and lymph nodes of unimmunized WT or *Ins1*^{eGFP} mice. Numbers indicate the percent of double tetramer-positive eGFPp:I-A^{b}-specific (double-tet^{+}) cells.

(b) Numbers of double-tet^{+} CD4^{+} T cells from pooled spleens and lymph nodes of unimmunized WT and *Ins1*^{eGFP} mice. Horizontal bars indicate geometric mean values and circles represent individual mice. Results are pooled from 5 experiments, n=16–17 total mice per group. (n.s. = not significant by unpaired t-test of $\log_{10}$ transformed data).

(c) Mean percent of double-tet^{+} CD4^{+} T cells from pooled spleens and lymph nodes of unimmunized WT or *Ins1*^{eGFP} mice that were CD44^{lo}. Data are pooled from 5 experiments, n=16–17 total mice per group. Error bars indicate standard deviations. (n.s. = not significant by unpaired t-test).

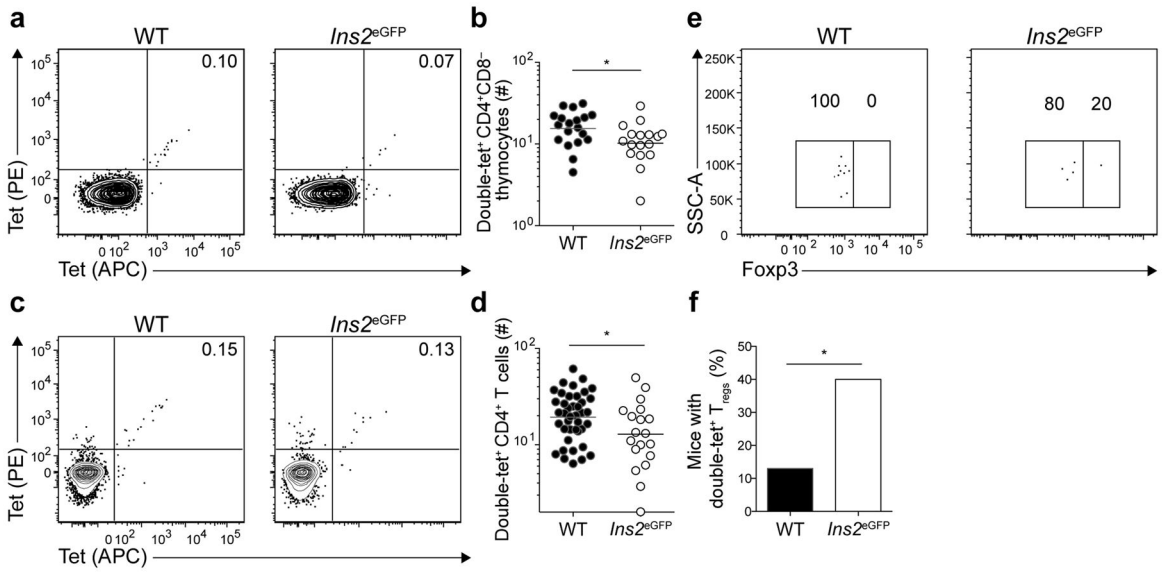

Figure 3. eGFPp:I-A^{b}-specific CD4^{+} T cells undergo limited clonal deletion in the thymus

(a) Contour plots of tet-PE versus tet-APC staining of tetramer-enriched CD4^{+}CD8^{-} thymocytes from WT or *Ins2*^{eGFP} mice.

(b) Numbers of double-tet^{+} CD4^{+}CD8^{-} thymocytes from WT and *Ins2*^{eGFP} mice. Results are pooled from 5 experiments, n=17–19 total mice per group. (* P<0.05 by unpaired t-test of $\log_{10}$ transformed data). Horizontal bars indicate geometric mean values and circles represent individual mice.

(c) Contour plots of tet-PE versus tet-APC staining of tetramer-enriched CD4^{+} T cells from pooled spleens and lymph nodes of unimmunized WT or *Ins2*^{eGFP} mice.

(d) Numbers of double-tet^{+} CD4^{+} T cells from pooled spleens and lymph nodes of WT or *Ins2*^{eGFP} mice. Results are pooled from 8 experiments, n=20–41 total mice per group. Horizontal bars indicate geometric mean values and circles represent individual mice. (* P<0.05 by unpaired t-test of $\log_{10}$ transformed data).

(e) Dot plots of Foxp3 expression by double-tet^{+} CD4^{+}CD8^{-} thymocytes from WT and *Ins2*^{eGFP} mice. Data are representative of samples from 5 independent experiments with n = 23 for WT mice and 20 mice for *Ins2*^{eGFP} mice.

(f) Frequency of mice with double-tet^{+} T_{reg} cells detected in the thymus. Data are pooled from 5 independent experiments with n = 23 for WT mice and 20 mice for *Ins2*^{eGFP} mice. (* P<0.05 by Chi-square test).

Numbers on each plot in (a), (c), and (e) indicate the percent of cells in the quadrant or gate.

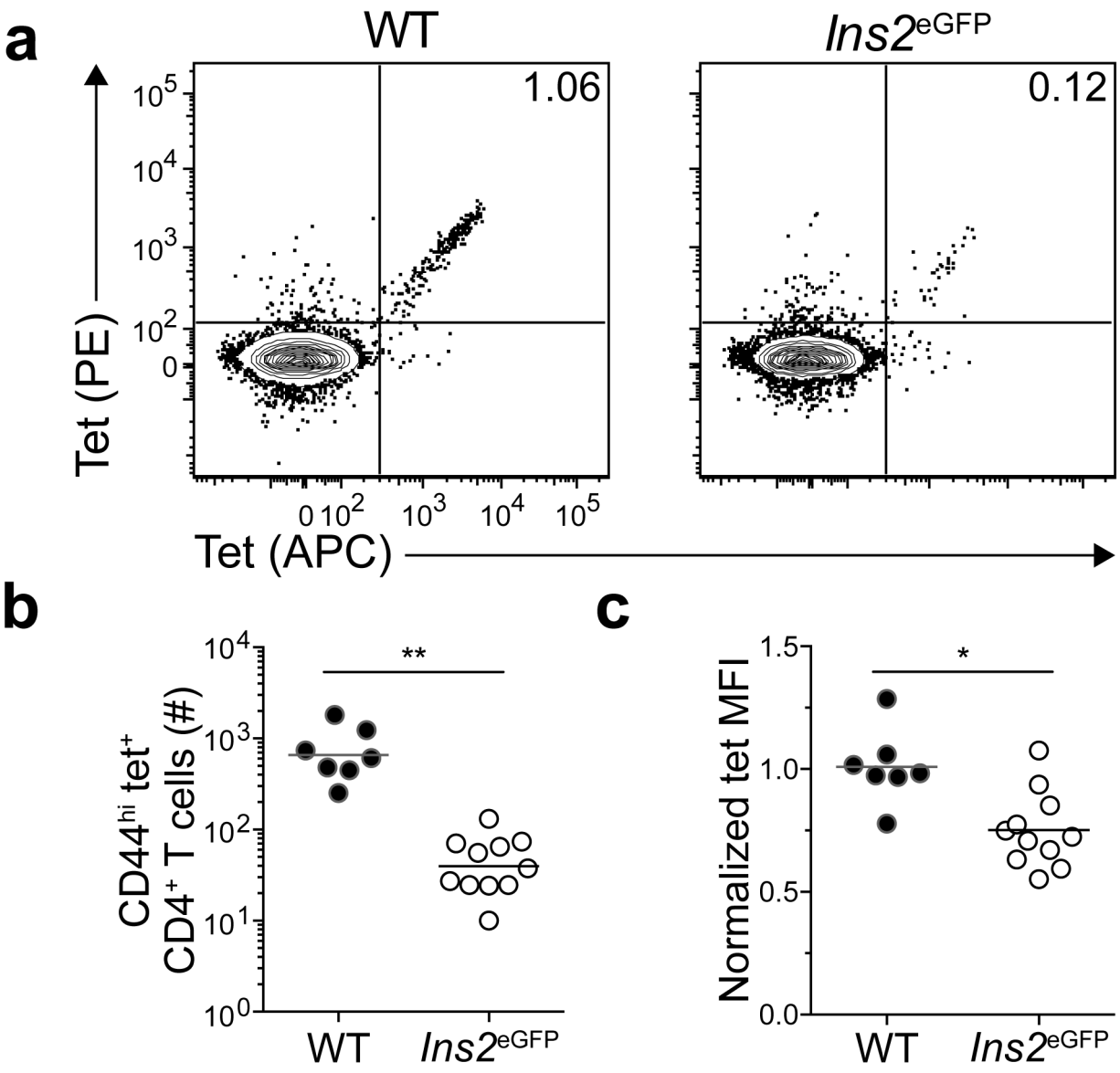

Figure 4. High affinity T cells are deleted in *Ins2*^{eGFP} mice

(a) Contour plots of tet-PE versus tet-APC staining of tetramer-enriched CD4$^+$ T cells from pooled spleens and lymph nodes of WT or *Ins2*^{eGFP} mice 6–7 days after infection with the Δ*actA*Δ*inlB* strain of *L. monocytogenes* (Lm-eGFP). Numbers indicate the percent of double-tet$^+$ cells.

(b) Numbers of CD44^{hi} tet$^+$ CD4$^+$ T cells from pooled spleens and lymph nodes of mice 6–7 days after infection with Lm-eGFP. Horizontal bars indicate geometric mean values and circles represent individual mice. Data are pooled from 3 independent experiments, n=7–11 total mice per group. (** P<0.0001 by unpaired t-test of $\log_{10}$ transformed data).

(c) Normalized tetramer mean fluorescence intensity (MFI) of cells identified in (b). MFIs within each experiment were normalized to those of WT controls. Horizontal bars indicate mean values and circles represent individual mice. Data are pooled from 3 independent experiments, n=7–11 total mice per group. (* P<0.005 by unpaired t-test).

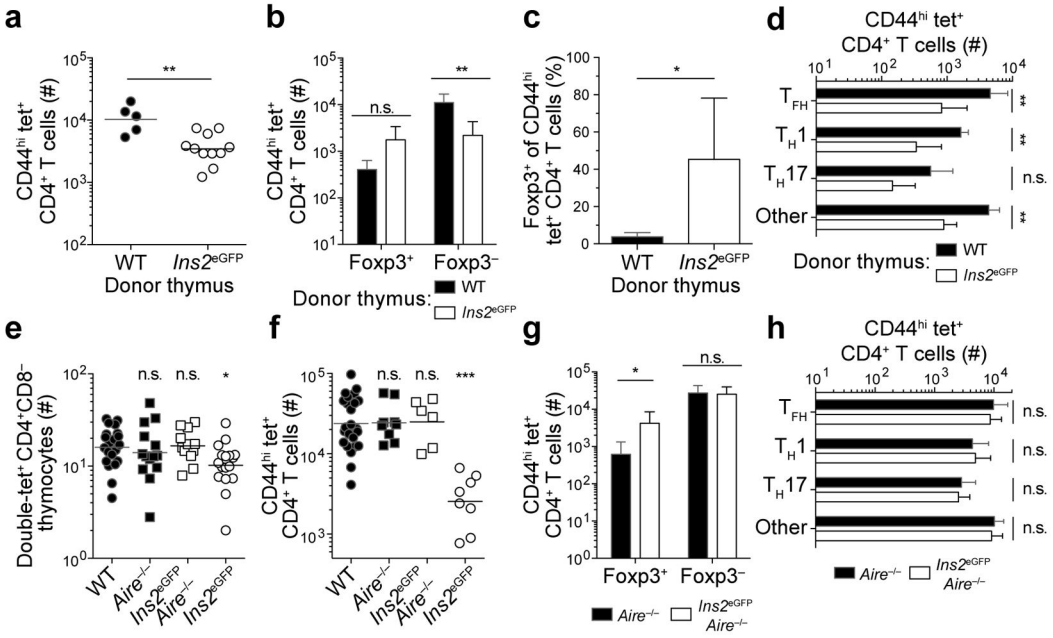

Figure 5. Aire-mediated thymic expression of eGFP promotes clonal deletion and T_{reg} induction in *Ins2*^{eGFP} mice

(a) Numbers of CD44^{hi} tet^{+} CD4^{+} T cells per B6-nude mouse 14 days after immunization with 100 μg of eGFPp in CFA. Mice received WT or *Ins2*^{eGFP} thymus grafts eight-twelve weeks before immunization, n=5–11 total mice per group.

(b) Numbers of CD44^{hi} tet^{+} CD4^{+} Foxp3^{+} T_{reg} cells and Foxp3^{-} effector T cells from mice in (a).

(c) Frequency of Foxp3^{+} T cells among cells identified in (a).

(d) Numbers of each Foxp3^{-} T effector cell subset in populations from (a).

(e) Numbers of double-tet^{+} CD4^{+}CD8^{-} thymocytes in WT, *Aire*$^{-/-}$, *Ins2*^{eGFP}*Aire*$^{-/-}$, and *Ins2*^{eGFP} mice. Cells were double-tetramer stained and analyzed as in Figure 2a. Data for WT and *Ins2*^{eGFP} mice are replotted from Figure 3b, n=12–21 total mice per group.

(f) Numbers of CD44^{hi} tet^{+} CD4^{+} T cells per mouse 14 days after immunization of WT, *Aire*$^{-/-}$, *Ins2*^{eGFP}*Aire*$^{-/-}$, and *Ins2*^{eGFP} mice with eGFPp in CFA. Data for WT and *Ins2*^{eGFP} mice are replotted from Figure 1a, n=6–23 total mice per group.

(g) Numbers of CD44^{hi} tet^{+} Foxp3^{+} T_{reg} cells and Foxp3^{-} effector T cells from mice in (f).

(h) Numbers of each Foxp3^{-} T effector cell subset among cells enumerated in (f). Data are from 2 (a–d), 6 (e), and 5 (f–h) independent experiments. Data are from pooled spleens and lymph nodes (a–d) and (f–h) or thymuses (e) of indicated mice. Horizontal bars indicate geometric means and symbols represent individual mice (a) and (e–f). Error bars indicate standard deviations in (b–d) and (g–h). * P<0.05, ** P<0.005, *** P<0.0001, n.s. = not significant by unpaired t-test of $\log_{10}$ transformed data (a–b), (d), (g–h); unpaired t-test (c); or one-way ANOVA of log10 transformed data (e–f).

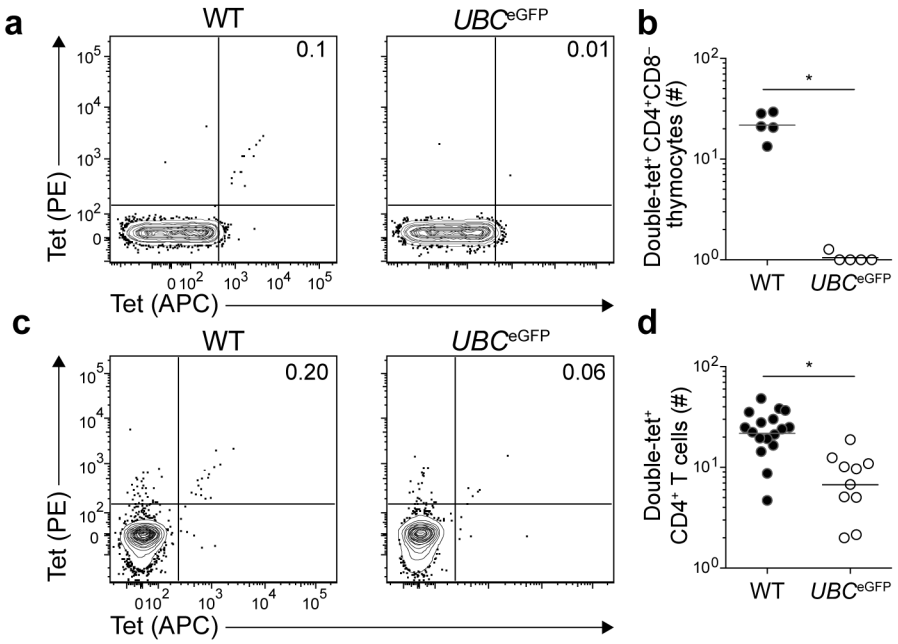

Figure 6. Expression of a self-epitope by thymic antigen-presenting cells induces intrathymic clonal deletion

(a) Contour plots of tet-PE versus tet-APC staining of tetramer-enriched $CD4^+CD8^-$ thymocytes from WT or *UBC*^{eGFP} mice.

(b) Number of $CD4^+CD8^-$ double-tet^+ cells in the thymuses of WT or *UBC*^{eGFP} mice. Horizontal bars indicate geometric mean values and circles represent individual mice. Data were pooled from two independent experiments, n=5 total mice per group. (* $P < 0.0001$ by unpaired t-test of $\log_{10}$ transformed data).

(c) Contour plots of tet-PE versus tet-APC staining of tetramer-enriched $CD4^+$ T cells from pooled spleens and lymph nodes of WT or *UBC*^{eGFP} mice.

(d) Number of $CD4^+$ double-tet^+ cells in pooled spleens and lymph nodes of WT or *UBC*^{eGFP} mice. Horizontal bars indicate geometric mean values and circles represent individual mice. Data were pooled from 4 independent experiments, n=10–17 total mice per group. Data for WT mice are replotted from Figure 2b. (* $P < 0.0001$ by unpaired t-test of $\log_{10}$ transformed data).

Numbers on each plot in (a) and (c) indicate the percent of double-tet^+ cells.

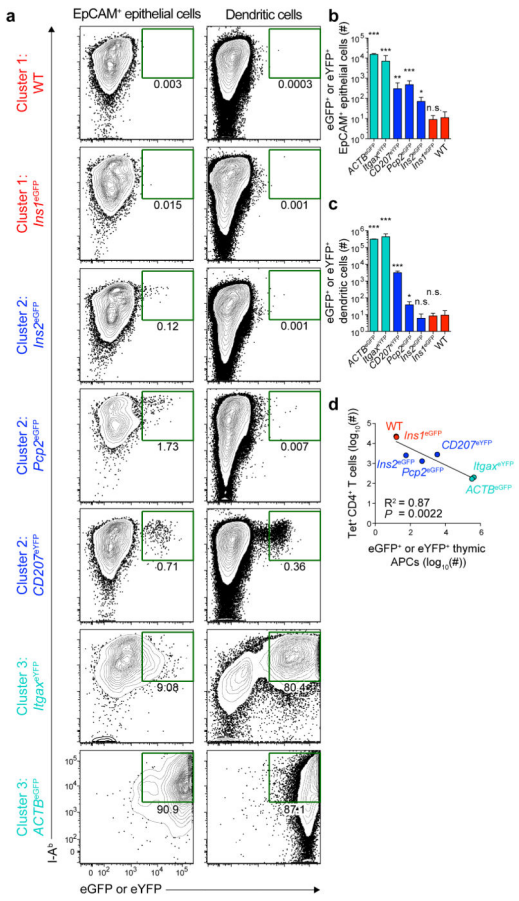

Figure 7. Frequency of self-antigen$^+$ thymic antigen-presenting cells correlates with the responsiveness of the corresponding CD4$^+$ T cell population

(a) Contour plots of MHCII (I-A^b) and eGFP$^+$ or eYFP$^+$ expression by EpCAM$^+$ thymic epithelial cells (left) and thymic dendritic cells (right) from the indicated members of Clusters 1–3. Plots are from 5 experiments. Numbers indicate the percent of cells that are I-A^{b+} and either eGFP$^+$ or eYFP$^+$.

(b) Numbers of eGFP$^+$ or eYFP$^+$ EpCAM$^+$ thymic epithelial cells in the indicated mouse strains, identified as in (a). Bars are colored according to the clusters identified in Figure 1d. Error bars represent the standard deviations. (n=3–6 total mice per group, * P<0.05, ** P<0.0005, *** P<0.0001, n.s. = not significant by one-way ANOVA of $\log_{10}$ transformed data).

(c) Numbers of eGFP$^+$ or eYFP$^+$ thymic dendritic cells in the indicated mouse strains, identified as in (a). Bars are colored according to the clusters identified in Figure 1d. Error bars represent the standard deviations. (n=3–6 total mice per group, * P<0.05, *** P<0.0001, n.s. = not significant by one-way ANOVA of $\log_{10}$ transformed data).

(d) Linear regression analysis of the $\log_{10}$(number of eGFP$^+$ or eYFP$^+$ thymic antigen-presenting cells) versus $\log_{10}$(number of tet$^+$ CD4$^+$ T cells 14 days after immunization). Each point represents values for an individual mouse strain as indicated. For each point, the y-axis value represents the $\log_{10}$(geometric mean from Figure 1a), and the x-axis value represents the $\log_{10}$(geometric mean for the total number of I-A^{b+} eGFP$^+$ or eYFP$^+$

EpCAM^{+} thymic epithelial cells and dendritic cells for each strain). Circles and labels are colored according to the clusters identified in Figure 1d.

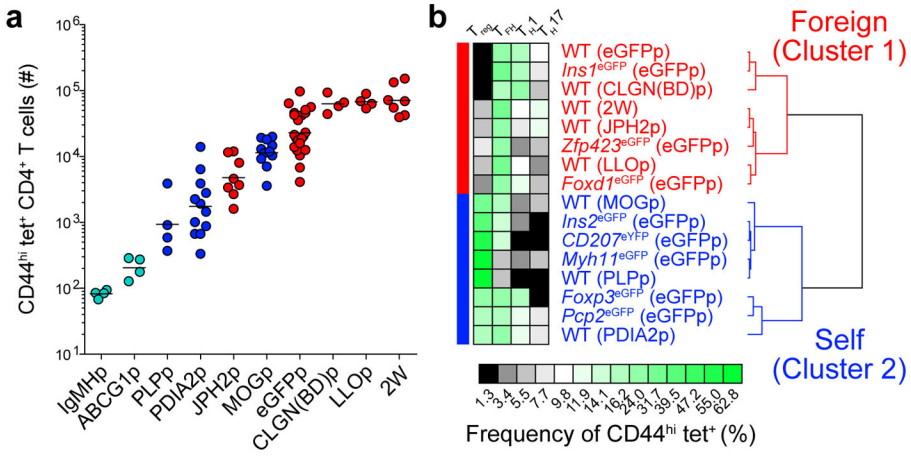

Figure 8. Tolerance mechanisms identified in eGFP expressing mouse strains govern tolerance to true self-antigens

(a) Numbers of CD44^{hi} peptide:I-A^{b+} (tet^{+}) CD4^{+} T cells from pooled spleens and lymph nodes of mice 13–14 days after immunization with 100 μg of each indicated peptide emulsified in CFA. Horizontal bars indicate geometric mean values. Data were pooled from 17 experiments, n=4–23 total mice per epitope. Circles represent individual mice and are colored according to the clusters identified in (b).

(b) Unsupervised hierarchical clustering of 16 self- and foreign- tet^{+} CD4^{+} T cell populations from (a). Profiles were clustered by percentage of cells of each subset as displayed in the heatmap. Two major clusters are indicated.